The magnetic sensitivity of the (250 − 278 nm) Fe II polarization spectrum.

David Afonso Delgado,[1,2] Tanausú del Pino Alemán,[1,2] and Javier Trujillo Bueno[1,2,3]

[1] *Instituto de Astrofísica de Canarias, E-38205 La Laguna, Tenerife, Spain*
[2] *Departamento de Astrofísica, Universidad de La Laguna, E-38206, La Laguna, Tenerife, Spain*
[3] *Consejo Superior de Investigaciones Científicas, Spain*

ABSTRACT

This paper presents a theoretical investigation on the polarization and magnetic sensitivity of the near-ultraviolet (near-UV) solar spectral lines of Fe II between 250 and 278 nm. In recent years, UV spectropolarimetry has become key to uncover the magnetism of the upper layers of the solar chromosphere. The unprecedented data obtained by the CLASP2 suborbital space experiment across the Mg II h and k lines around 280 nm are a clear example of the capabilities of near-UV spectropolarimetry for the magnetic field diagnostics throughout the whole solar chromosphere. Recent works have pointed out the possible complementary diagnostic potential of the many Fe II lines in the unexplored spectral region between 250 and 278 nm, but no quantitative analysis of the polarization and magnetic sensitivity of those spectral lines has been carried out yet. To study the polarization signals in these spectral lines, we create a comprehensive atomic model including all the atomic transitions resulting in strong spectral lines. We then study the magnetic sensitivity of the linear and circular polarization profiles in a semi-empirical model representative of the quiet sun. We present a selection of Fe II spectral lines with significant linear and circular polarization signals and evaluate their diagnostic capabilities by studying their formation heights and magnetic sensitivity through the action of the Hanle and Zeeman effects. We conclude that when combined with the CLASP2 spectral region these Fe II lines are of interest for the inference of magnetic fields throughout the solar chromosphere, up to near the base of the corona.

Keywords: Spectropolarimetry, Radiative Transfer, Solar magnetic fields, Quiet Sun chromosphere

1. INTRODUCTION

Spectral lines encode information about the physical conditions of the emitting plasma. Therefore, the study of their formation in given models of the solar atmosphere is very important for reaching the goal of inferring its physical properties from the observed spectral line radiation. In particular, the linear and circular polarization profiles carry information about the magnetic field strength and geometry in the their region of formation. Even though the solar spectrum is populated by plenty of spectral lines forming everywhere in the solar atmosphere, it is in the ultraviolet (UV) region of the spectrum where we find abundant spectral lines forming in the solar chromosphere and transition region. Determining the magnetic field in these regions of the upper solar atmosphere is of fundamental importance for understanding how the energy is transported from the underlying layers and dissipated in the chromosphere and the corona, where the explosive events that can impact the heliosphere take place. For these reasons, ultraviolet spectropolarimetry is increasingly recognized as a key diagnostic tool for facilitating new breakthroughs in our empirical understanding of solar and stellar magnetic fields(e.g., the review of Trujillo Bueno & del Pino Alemán 2022).

The *Interface Region Imaging Spectrograph* (IRIS, De Pontieu et al. 2014) mission is one of the main examples of the relevance of UV spectroscopy for investigating the upper layers of the solar atmosphere. IRIS has been in operation since 2013 measuring the intensity profiles in several windows of the UV solar spectrum, including spectral lines such as Mg II h and k (279.6 and 280.3 nm), C II (133.4/133.5 nm), or Si IV (139.4/140.3 nm). The research exploiting the data provided by the IRIS mission has significantly improved our knowledge about the solar chromosphere (see De Pontieu et al. 2021).

Concerning UV spectropolarimetry, the most recent relevant advances are the *Chromospheric Lyman-Alpha SpectroPolarimeter* (CLASP, Kobayashi et al. 2012), which in 2015 observed the intensity and linear polarization of the H I

dafonso@iac.es

Ly α line (Kano et al. 2017; Trujillo Bueno et al. 2018), and the *Chromospheric LAyer SpectroPolarimeter* (CLASP2, Song et al. 2022), which in 2019 acquired unprecedented spectropolarimetric data of the 279.2 - 280.7 nm near-UV spectral region that contains the Mg II h and k lines and several other lines of great diagnostic interest (Ishikawa et al. 2021; Rachmeler et al. 2022). These suborbital space missions were motivated by a series of theoretical investigations (see Trujillo Bueno et al. 2011, 2012; Belluzzi et al. 2012; Belluzzi & Trujillo Bueno 2012; Alsina Ballester et al. 2016; del Pino Alemán et al. 2016), which predicted that the polarization signals are measurable and magnetically sensitive and showed the importance of the effects of partial frequency redistribution (PRD), J-state interference, and the joint action of the Hanle, Zeeman, and magneto-optical effects on the linear polarization signals produced by scattering processes. Moreover, the analysis of the circular polarization profiles measured by CLASP2 in the resonance lines of Mg II and Mn I allowed for the first mapping of the longitudinal component of the magnetic field from the photosphere to the upper chromosphere, just below the transition region (Ishikawa et al. 2021; Li et al. 2023).

Despite all these novel advances, there are still many unexplored regions in the UV spectrum of the Sun. The polarization signals of the near-UV Fe II spectral lines that are located blueward of the CLASP2 spectral region have been proposed as potentially useful for facilitating the exploration of chromospheric magnetism (Judge et al. 2021). In particular, in the 250 - 278 nm spectral window we can find many lines belonging to this ion, including a strong resonant multiplet at 260 nm. Due to the lack of spectroscopic or spectropolarimetric solar observations in this spectral region, previous works found in the literature are mainly focused on the study of the intensity spectrum of these spectral lines in other stars (Judge & Jordan 1991; Judge et al. 1992) or of other Fe II spectral lines located in observed spectral regions, such as the small Fe II emission line in the red wing of the Ca II line at 369.94 nm (Cram et al. 1980; Watanabe & Steenbock 1986). Moreover, as far as we know, there are not theoretical investigations about the polarization signals of these spectral lines or about their magnetic sensitivity.

In this work we present the first detailed theoretical study on the polarization and magnetic sensitivity of the Fe II lines that are located in the 250 - 278 nm near-UV spectral region, as well as their suitability to infer magnetic fields in the solar atmosphere. In Sec. 2 we introduce the methods and tools used in our radiative transfer modeling. The atomic model used in the calculation is described in Sec. 3. In Sec. 4 we show the results of our modeling, including a selection of the most interesting spectral lines, following certain criteria, as well as an analysis of their magnetic sensitivity and suitability to infer magnetic fields in the solar atmosphere. Finally, present our conclusions in Sec. 5.

2. FORMULATION OF THE PROBLEM

To study the formation and magnetic sensitivity of the Fe II lines in the spectral window between 250 and 278 nm we solve the problem of generation and transfer of polarized radiation in optically-thick magnetized plasmas out of local thermodynamic equilibrium (NLTE). This problem is both non-local and non-linear, requiring the simultaneous solution of the atomic excitation (populations of the atomic substates and quantum coherence between them) described by the statistical equilibrium equations (SEE) and of the radiation propagation throughout the atmosphere governed by the radiative transfer (RT) equations. We solve this problem by applying the HanleRT code (del Pino Alemán et al. 2016, 2020) to a 1D plane-parallel model of the solar atmosphere. We have chosen the semi-empirical C model of the quiet Sun described in Fontenla et al. (1993, hereafter FAL-C).

Even though PRD effects and quantum interference can have an impact on the linear scattering polarization profiles (e.g., Casini et al. 2017), we neglect both for the following reasons: first, these effects are particularly relevant in the far wings of these spectral lines and, as we discuss in more detail in Sec. 3, in the near-UV region of the solar spectrum the effect of spectral line blanketing is notably strong, masking the impact of these effects and making the use of the line wings for atmospheric diagnostic extremely difficult. Second, including these physical ingredients has a significant computational cost, especially when considering the size of the atomic model needed to study all the spectral lines considered in this work. For these reasons, the calculations shown in this paper assume complete frequency redistribution (CRD) and neglect quantum interference between the substates pertaining to different atomic levels, which are often good approximations to model the spectral line core.

3. ATOMIC MODEL

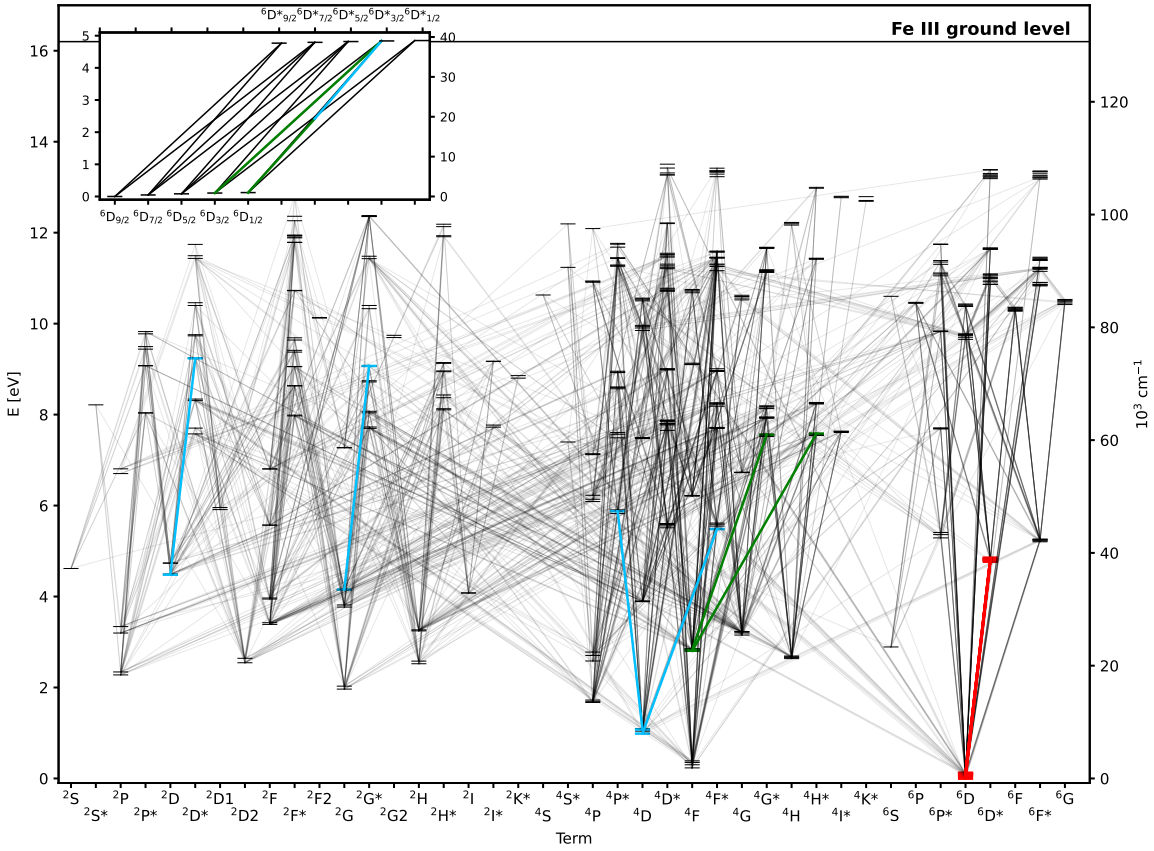

Figure 1. Grotrian diagram of the Fe II atom considered in this work. The red line indicates the resonant multiplet at 260 nm, shown with further detail in the Grotrian diagram in the inset at the upper-left. The blue (green) lines indicate the transitions shown in Fig. 6 (Fig. 8).

As far as we know, there are not previous studies on the formation of the Fe II polarization profiles in the spectral window between 250 and 278 nm and, therefore, on the atomic model necessary to reliably model the polarization of all these spectral lines. Consequently, the first step is to build a suitable atomic model including all the atomic transitions that could produce (or impact) any interesting polarization signal in the spectral region of interest.

In the solar chromosphere the iron atoms are mostly singly ionized, and, consequently, Fe II is the dominant ion (e.g., Shchukina & Trujillo Bueno 2001). Our atomic model thus includes just the Fe II levels and the ground level of Fe III. We take the atomic level energies and the Einstein coefficients for spontaneous emission from the NIST database (Kramida 2013). We approximate the photoionization cross sections as hydrogenic (Mihalas 1978). The rates of ionizing inelastic collisions with electrons are calculated using the approximation of Allen (1963). The rate of excitation due to inelastic collisions with electrons are calculated following van Regemorter (1962) for pairs of levels fulfilling the electric dipole selection rules, and following Bely & van Regemorter (1970) for pairs of levels that do not fulfill those selection rules. The rate of depolarizing collisions with neutral hydrogen atoms are calculated assuming the Van der Waals potential (Lamb & Ter Haar 1971; Landi Degl'Innocenti & Landolfi 2004). We neglect inelastic collisions with hydrogen atoms.

In our atomic model we only include those transitions with a spontaneous emission probability above a certain threshold ($A_{ul} \geq 10^6$ s^{-1}), which can produce a significant (in terms of its depths in the emergent spectrum) spectral line. Moreover, once we have solved the self-consistent RT problem with the whole atomic model we then remove one third of the levels, the least populated ones, as well as those not radiatively connected with any other atomic

level. Using the reduced atomic model results in relative differences of no more than 5% at the center of the emergent intensity profiles for the spectral lines in the 250 – 280 nm range.

Our atomic model to study the formation and polarization of the Fe II spectral lines between 250 and 278 nm has 453 Fe II atomic levels (and the ground level of Fe III) and 2225 radiative transitions. The model is thus complete enough to ensure a reliable calculation of the population balance of the levels involved in the formation of any of the spectral lines in the range between 250 and 280 nm.

In Fig. 1 we show the Grotrian diagram for the described atomic model, including all the radiative transitions. The red line in the diagram indicates the resonant multiplet that produces a series of intense spectral lines around 260 nm. A detailed Grotrian diagram of this multiplet is shown in the inset at the top-left corner of Fig. 1. The blue and green lines highlight some spectral lines analyzed in detail in Secs. 4.1 and 4.2.

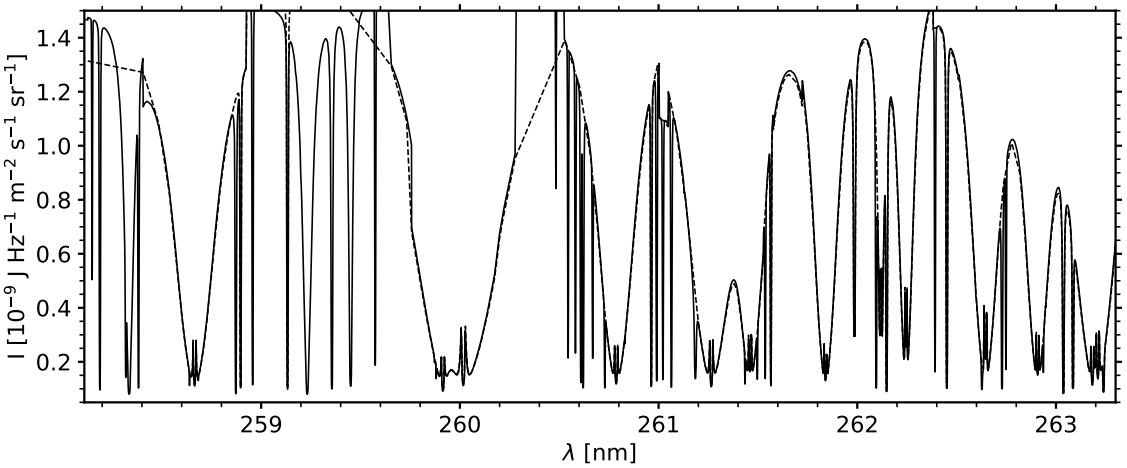

Figure 2. Intensity profile in the spectral region of the Fe II resonant multiplet around 260 nm. Solid line: atomic model with 453 levels. Dashed line: atomic model with 90 levels.

The rates of inelastic collisions are critical for the population balance of the Fe II atomic levels (Judge et al. 1992). To build our atomic model we use very rough approximations to these rates, what can have a significant effect on the emergent Stokes profiles. In order to study how the inelastic collisions affect the emergent profiles, we create a reduced Fe II atomic model with 90 levels (including the Fe III ground level) and 113 radiative transitions, which can correctly model the emergent intensity profiles of the resonant multiplet around 260 nm; that is, it is able to reproduce the same emergent intensity profiles for these strong resonant lines (Fig. 2). Using the reduced model, we perform different numerical experiments in which we multiply the inelastic collisional rates between pairs of atomic levels fulfilling (not fulfilling) the electric dipole selection rules with a factor Ω_A (Ω_F).

Due to the lack of solar spectroscopic observations, it is not possible to compare our calculations with the solar spectrum at these wavelengths. We have thus opted for a comparison with the flux of a solar analog star, α Cen A, a very close G2V star (Torres et al. 2006), the same spectral type than the Sun. We compare the intensity flux profile of α Cen A[1] observed with the *Space Telescope Imaging Spectrograph* (STIS, Woodgate et al. 1998) on board of the *Hubble Space Telescope* (HST) with calculations in the FAL-C model for different values of Ω_A and Ω_F (Fig. 3). The first evident difference between the theoretical and observed fluxes is the significantly diminished continuum intensity in the observation, showing considerably wider lines. The large amount of spectral lines in the UV spectrum, contributing to the opacity, produce the so called UV blanketing, which consistently reduces the intensity flux across the spectral region, giving the impression of a much lower continuum and of wider spectral lines. Consequently, we focus our analysis to the core and near wings of the Fe II spectral lines.

With the inelastic collisions given by the above-mentioned approximations ($\Omega_A = \Omega_F = 1.0$; blue curve) the flux in the line core is significantly larger than the observed flux, with significant emission features in the near wings which are absent in the observation. We find the best agreement when all the inelastic collisional rates are reduced by a factor

[1] This spectrum is available in The Advanced Spectral Library Project (ASTRAL, https://archive.stsci.edu/prepds/astral/). For further details see Ayres (2013, 2010)

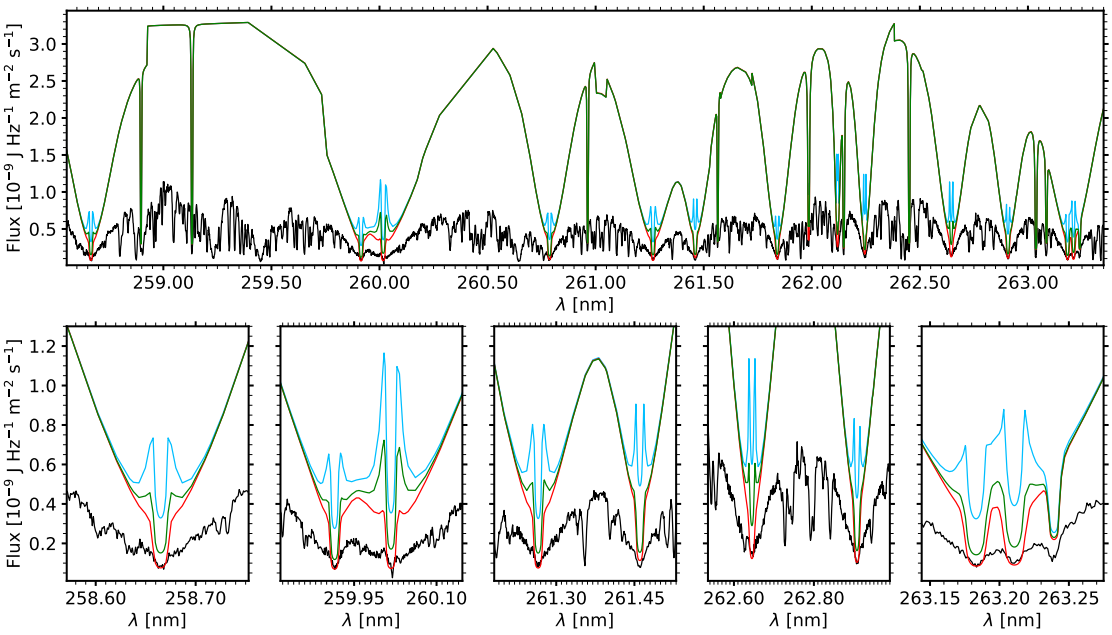

Figure 3. Emergent intensity flux profile in the spectral region of the Fe II resonant multiplet at 260 nm. The black curve shows the flux of α Cen A (a G2V star) measured with the STIS instrument of the HST. Each colored curve shows the flux profile calculated with different inelastic collisional rates, resulting by scaling the original atomic model values (see Sec. 3) by Ω_A (Ω_F) for pairs of levels that fulfill (do not fulfill) the electric dipole selection rules: $\Omega_F = \Omega_A = 1$ (blue), $\Omega_F = 0.1$ and $\Omega_A = 1$ (green), and $\Omega_F = \Omega_A = 0.1$ (red). The bottom row shows in more detail the core of the strongest transitions.

of ten ($\Omega_A = \Omega_F = 0.1$; red curve); the intensity flux at the line cores becomes remarkably similar to the observed flux and the near wing emission features completely vanish (see bottom row of Fig. 3). Our atomic model is thus able to adequately reproduce the intensity flux of the most intense Fe II atomic lines in the near-UV spectrum of a solar-like star.

4. RESULTS

We use the atomic model described in Sec. 3 to model the Stokes profiles of the Fe II atomic lines in the UV spectral window between 250 and 278 nm. In particular, we study their linear and circular polarization profiles and their capability to uncover the magnetic fields of the solar atmosphere. For this purpose, we perform RT calculations including scattering polarization and the Hanle and Zeeman effects assuming CRD. We study the fractional linear polarization signals for a line-of-sight (LOS) near the solar limb ($\mu = \cos\theta = 0.1$, with θ the heliocentric angle). We then impose different magnetic fields to investigate the magnetic sensitivity of their linear polarization. Finally, we study the formation of Zeeman-induced circular polarization signals for the disk center LOS. We then study the suitability of the weak-field approximation (WFA) to infer the longitudinal component of the magnetic field (B_L) from the circular polarization.

4.1. *Linear Polarization Signals.*

Fig. 4 shows the fractional linear polarization Q/I profile in the unmagnetized FAL-C model atmosphere for the spectral region of the Fe II resonant multiplet around 260 nm for the LOS at $\mu = 0.1$ (see blue curve in Fig. 4). While some of the strongest lines, in terms of their absorption features in the intensity profile, hardly show any significant linear polarization signal (see lines at 259.914, 261.265, or 261.840 nm) others exhibit relatively large signals shown in detail in the bottom panels of Fig. 4. The colored background in Fig. 4 shows the logarithm of the normalized contribution function for Stokes Q, which gives a measure of how much each height layer in the model atmosphere contributes, at each wavelength, to the linear polarization of the emergent radiation. The red and blue colors indicate positive or negative contributions, respectively. We can conclude, from the contribution function, that the linear polarization at the line core of the lines shown in the figure is formed between the middle and upper chromosphere (above ≈ 1 Mm in the FAL-C model).

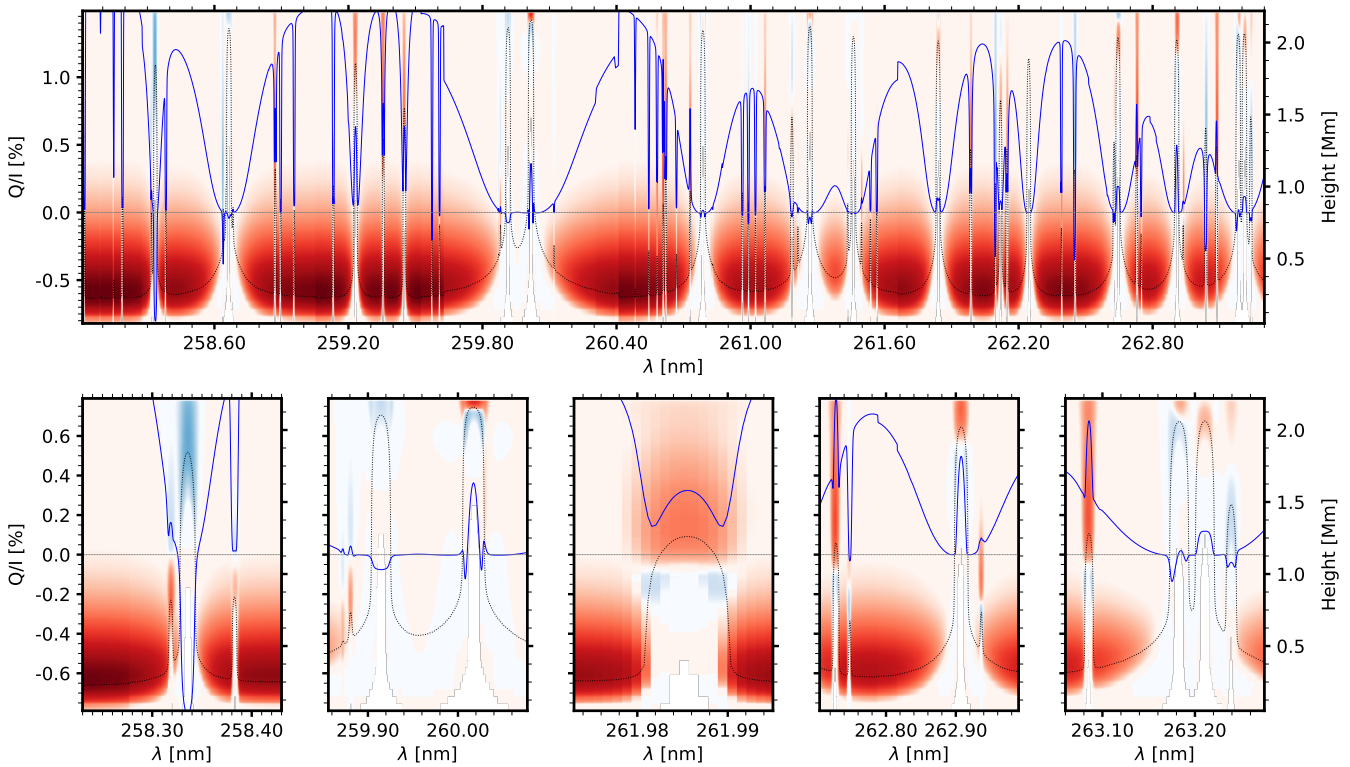

Figure 4. Fractional linear polarization profile Q/I (solid blue curve, left plot axes) and height where the optical depth is equal to one (dotted black curve, right plot axes) in the spectral region of the Fe II resonant multiplet around 260 nm. The colored background shows the logarithm of the normalized contribution function for Stokes Q (with the red and blue colors indicating positive and negative contributions, respectively). Details around some of the lines with the strongest Q/I signals are shown in the bottom row.

We have selected the spectral lines with zero-field scattering polarization signals $Q/I > 0.2$ % at the line core, and we have analyzed their magnetic sensitivity in order to determine which ones are suitable for the diagnostics of chromospheric magnetic fields. In the left panel of Fig. 5 we show the height where the optical depth is unity at the line center (which gives an idea of the region of formation) for the selected lines, as well as their Hanle critical field (B_H), their line center zero-field Q/I signal, and information about the blends with neighbor lines. The Hanle critical field is the magnetic field strength for which the Zeeman splitting equals the natural width of the line (e.g., Trujillo Bueno 2001):

$$B_H = \frac{1.137 \cdot 10^{-7}}{t_{\rm life} g}, \tag{1}$$

with $t_{\rm life}$ and g the radiative lifetime and Landé factor of the line level under consideration, respectively. Typically, a spectral line is sensitive, via the Hanle effect, to magnetic fields with strengths between approximately $0.2B_H$ and $5B_H$.

To characterize the blends with other spectral lines we compare the theoretical and observed fluxes from Fig. 2 with a synthetic profile including all the transitions from the Kurucz database in LTE (Kurucz & Bell 1995), similarly to the approach of Judge et al. (2021). Through visual inspection, we look for any spectral line close enough to the selected Fe II line to affect their profiles, and we classify them in three categories: no nearby blends (circles in Fig. 5), a moderate blend in the wings, far enough from the line core (squares), or a significant blend close to the line core (diamonds). Many of the selected lines show a nearby blend but, in these cases, the line core (line region sensitive to the Hanle effect) should not be affected significantly.

Most of the spectral lines in our selection form in the middle chromosphere (around 1.25 Mm in the FAL-C semi-empirical model). A relatively small number of lines form in the lower chromosphere and near the FAL-C temperature minimum (around 0.5 Mm). Moreover, several stronger lines form in the upper chromosphere (above around 1.8 Mm).

Table 1. Wavelength, level configuration and energy, Einstein coefficient for spontaneous emission, and critical Hanle magnetic field of the upper level for the spectral lines studied in detail in Sec. 4.1.

λ [nm]	Transition	Energies [cm^{-1}]	A$_{ul}$ [10^8 s^{-1}]	B$_H^u$ [G]
260.609	b^{2}D$_{3/2}$ - x^{2}D$^o_{3/2}$	36 126 - 74 498	2.00	∼40
252.257	c^{2}G$_{7/2}$ - w^{2}G$^o_{7/2}$	33 501 - 73 143	2.60	∼57
258.336	a^{4}D$_{3/2}$ - z^{4}P$^o_{3/2}$	8 680 - 47 389	0.88	∼20
262.908	a^{6}D$_{1/2}$ - z^{6}D$^o_{3/2}$	977 - 39 013	0.87	∼16
275.655	a^{4}D$_{7/2}$ - z^{4}F$^o_{9/2}$	7 955 - 44 232	2.20	∼22

These latter transitions belong to a resonant multiplet (260.017 and 262.907 nm) and the metastable multiplets a^4D - z^4P° (258.336 and 259.231 nm), a^4D - z^4D° (274.035 nm), and a^4D - z^4F° (274.730, 275.013 and 275.658 nm).

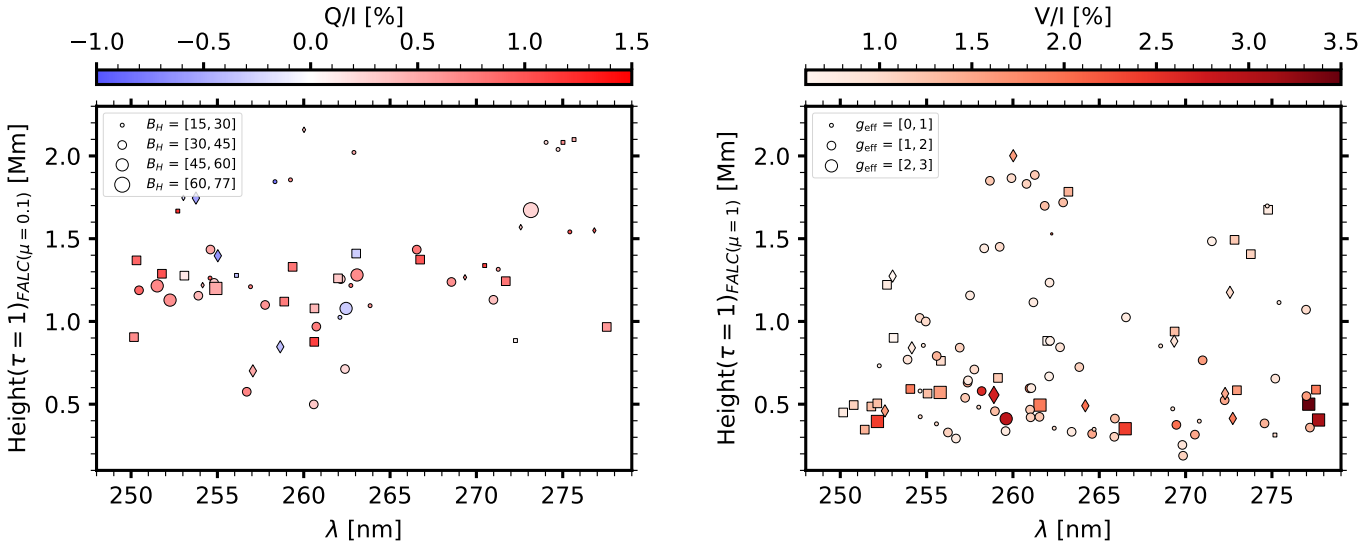

Figure 5. The left (right) panel shows a selection of the Fe II spectral lines with larger fractional linear (circular) polarization Q/I (V/I) signals for the LOS at $\mu = 0.1$ ($\mu = 1$). The size of the markers indicates the critical Hanle field B_H (the effective Landé factor $g_{\rm eff}$) for each spectral line. The color shows the amplitude of the Q/I (V/I, for a longitudinal magnetic field of 50 G) signals for each spectral line. The markers's shape indicate the presence and significance of blends with other spectral lines: circle = no blends, square = moderate blend, and diamond = severe blend (see text for further details).

Most of the lines in our selection have critical Hanle fields below 50 G and, for those lines forming in the upper chromosphere, we always find $B_H < 30$ G. Consequently, these spectral lines are thus expected to be sensitive to magnetic fields with strengths considerably smaller than 100 G and, for those lines forming in the upper chromosphere, to magnetic fields around 20 G or less. These magnetic field strengths are of the order we expect for the chromospheric magnetic field in the quiet Sun and, therefore, these spectral lines seem to be good candidates to study the quiet Sun magnetism in the upper chromosphere.

To actually study the magnetic sensitivity of these spectral lines, we have selected five specific cases, choosing lines forming in different layers of the solar atmosphere and with different Hanle critical fields. Table 1 summarizes the atomic data of the five chosen transitions, also highlighted in blue in the Grotrian diagram of Fig. 1. In the FAL-C model we impose a horizontal magnetic field ($\theta_{\rm B} = 90^\circ$, $\phi_{\rm B} = 0$, with $\theta_{\rm B}$ and $\phi_{\rm B}$ the polar and azimuthal angles of the magnetic field vector with respect to the local vertical) with different strengths, and we compare the calculated Q/I profiles of the radiation emerging at the $\mu = 0.1$ LOS (see Fig. 6): 0 (black), 10 (blue), 20 (green) and 50 G (red).

The background color in Fig. 6 shows the logarithm of the normalized contribution function as in Fig. 4, what confirms that the linear polarization in this selection of lines form at different heights ranging from a few hundred kilometers above the temperature minimum (> 0.5 Mm) and the upper chromosphere ($\gtrapprox 1.7$ Mm). For the two metastable transitions at 260.608 and 252.257 nm (first and second panels in Fig. 6) most of the contribution is localized in a relatively extense region in the middle chromosphere of the model. These two transition have $B_H = 40$ and 50 G, respectively and, consequently, a magnetic field of just 10 G already induces a significant depolarization of the line core linear polarization. A magnetic field of 50 G already reduces the fractional linear polarization by more than a factor ten.

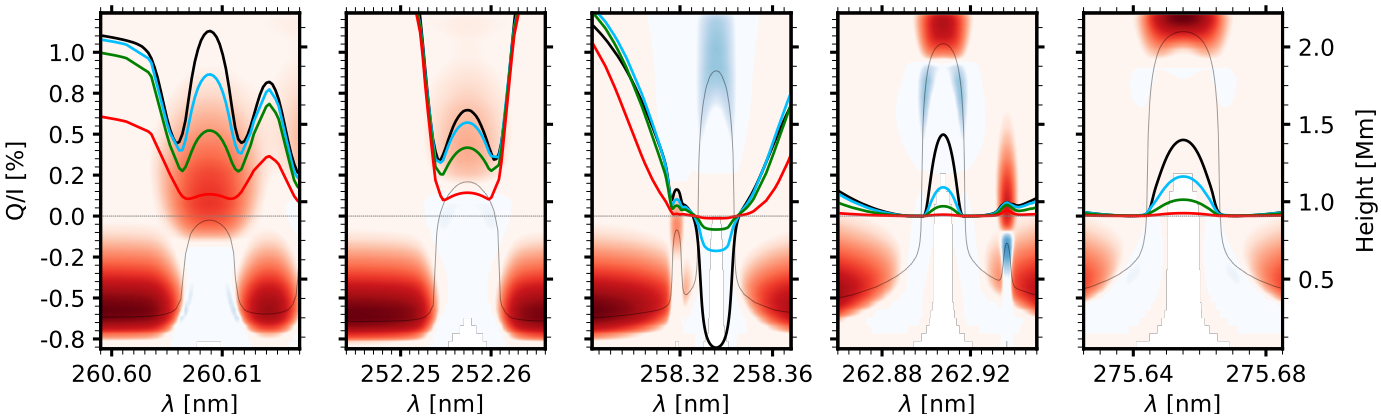

Figure 6. Like in Fig. 4, but for the five selected spectral lines (see Tab. 1) for the LOS at $\mu = 0.1$. The color of the curve indicates the strength of a horizontal ($\theta_B = 90°$, $\phi_B = 0$) and homogeneous magnetic field in the FAL-C model: 0 (black), 10 (blue), 20 (green), and 50 G (red).

Contrarily to the rest of the selected transitions, the spectral line at 258.336 nm shows a strong negative fractional linear polarization signal (radial polarization; see third panel of Fig.6) of about -0.8 %. This line forms in a extense region of the upper chromosphere of the model and it has $B_H \approx 20$ G. Consequently, a 10 G magnetic field already more than halved the amplitude of the linear polarization and it is dramatically depolarized by a 50 G magnetic field.

Finally, regarding the spectral lines at 262.908 and 275.655 nm, their line core linear polarization forms in a narrow area in the top of the FAL-C model's chromosphere (between 1.9 and 2.2 Mm and between 2.0 and 2.2 Mm, respectively). Their critical Hanle fields are also relatively small (16 and 22 G, respectively), as evident from the strong depolarization induced by a magnetic field of 20 G (see fourth and fifth panels of Fig. 6). Nevertheless, these lines are sensitive to magnetic fields with strengths of a few gauss, of the order of the typical magnetic field strengths expected in the upper chromosphere of the quiet Sun. Moreover, note that the chosen magnetic field geometry, namely horizontal with respect to the local vertical, is such that it maximizes the depolarization of the fractional linear polarization Q/I profiles.

4.2. *Circular Polarization Signals.*

We now study the circular polarization profiles of the Fe II UV lines and their suitability to infer the longitudinal component of the magnetic field via the WFA.

For this purpose, we calculate the fractional circular polarization profiles V/I for a LOS at the disk center ($\mu = 1$), imposing in the FAL-C model a uniform vertical magnetic field of 50 G. We show in the right panel of Fig. 5 those lines with a circular polarization amplitude above 0.5%, with the color of the marker indicating such amplitude and its size indicating the effective Landé factor ($g_{\rm eff}$) calculated assuming L-S coupling. Although the lobes of the circular polarization profiles typically sample the atmosphere at regions significantly below those sampled by the line cores, we will use the height at which the line-center optical depth is unity to indicate the approximate height at which these profiles are formed.

A total of 103 spectral lines show circular polarization signals larger than 0.5 %. Most of these lines form between the upper photosphere and lower chromosphere. A considerable amount of Fe II lines in the selection form in the middle and upper chromosphere, e.g., the transitions of the resonant multiplet a^6D - z^6D°.

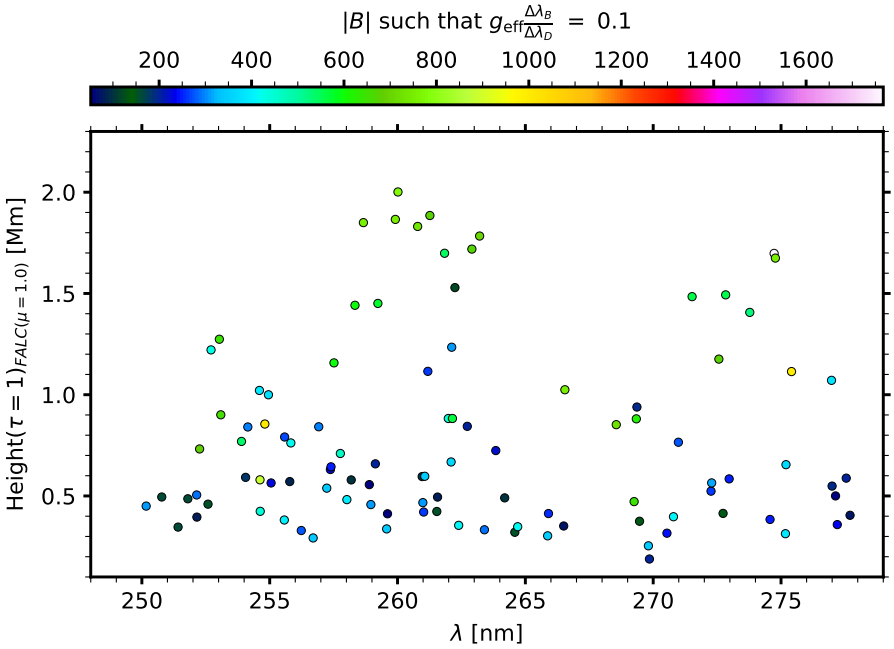

Figure 7. Magnetic field strength for each selected spectral line (see right panel of Fig. 5) such that $g_{\rm eff}\frac{\Delta\lambda_B}{\Delta\lambda_D} = 0.1$. $\Delta\lambda_D$ is calculated for the temperature and microturbulent velocity in the model atmosphere at the height where the optical depth at the line core is equal to one. This gives an idea of the magnetic field up to which the weak-field condition is fulfilled for each spectral line.

Given the computational demands for solving the full NLTE RT problem, it is ideal to have inference methods that allow for a quick determination of the magnetic field without the need of carrying out the NLTE modeling of the observations. The WFA, if suitable, allows for the very quick determination of the longitudinal component of the magnetic field (e.g., for the Mg II h and k lines, see Afonso Delgado et al. 2023). For this approximation to be suitable, the line's Doppler width ($\Delta\lambda_D$) must be much larger than the magnetic Zeeman splitting between the atomic magnetic sublevels ($\Delta\lambda_B$),

$$g_{\rm eff}\frac{\Delta\lambda_B}{\Delta\lambda_D} << 1, \tag{2}$$

where $\Delta\lambda_B = 4.6686 \cdot 10^{-13} B\lambda_0^2$ (with B in Gauss and λ_0 in Å) and $\Delta\lambda_D = \frac{\lambda_0}{c}\sqrt{\frac{2kT}{m} + v_m^2}$ (with T and v_m the temperature and turbulent velocity in the formation region of the line, with c the speed of light, k the Boltzmann constant, and m the mass of the atom). In this way, we can roughly expect the WFA to be valid when the magnetic field strength is below the value which makes $g_{\rm eff}\frac{\Delta\lambda_B}{\Delta\lambda_D} = 0.1$. Fig. 7 shows the maximum magnetic field strength for which this condition is fulfilled. The included lines are those selected in the right panel of Fig. 5.

For those spectral lines whose line core forms between the middle and upper chromosphere the WFA is valid, through the chosen criteria, for any magnetic field strength below 500 G (except for the one spectral line at 262.245 nm). We can thus be confident that the WFA necessary condition is met both in quiet sun regions and in the weaker manifestations of active regions, such as plages.

For spectral lines originating between the upper photosphere and lower chromosphere we can distinguish two cases: spectral lines in which the WFA applicability condition is met for $B_L <= 200$ G, and thus only applicable in quiet Sun regions, and spectral lines for which the applicability condition is $B_L <= 600$ G, and thus it can also be applied in relatively weak active regions such as plages.

To study in detail the actual applicability of the WFA to infer the longitudinal magnetic field, we select four spectral lines, relatively close in wavelength, and infer the magnetic field from a theoretical circular polarization profile calculated in the FAL-C model imposing a certain magnetic field stratification. Table 2 summarizes the atomic data of the four chosen transitions, also highlighted in green in the Grotrian diagram of Fig. 1. Among these spectral lines

Table 2. Wavelength, level configuration and energy, Einstein coefficient for spontaneous emission, and effective Landé factor for the spectral lines studied in detail in Sec. 4.2

λ [nm]	Transition	Energies [cm^{-1}]	A$_{ul}$ [10^7 s^{-1}]	g$_{\rm eff}$
259.608	b^{4}F$_{9/2}$ - z^{4}H$^{\rm o}_4$	22 637 - 61 156	0.12	2.5
262.148	b^{4}F$_4$ - z^{4}G$^{\rm o}_4$	22 810 - 60 956	3.40	1.1
262.119	a^{6}D$_{3/2}$ - z^{6}D$^{\rm o}_3$/2	862 - 39 013	0.43	1.9
262.908	a^{6}D$_{1/2}$ - z^{6}D$^{\rm o}_3$/2	977 - 39 013	8.70	1.5

we find two resonant transitions (262.119 and 262.908 nm) and two transitions with metastable lower levels in the b^{4}F term (259.608 and 262.148 nm).

The dotted curves in the first and second column in Fig. 8 show the fractional circular polarization profile of the radiation emerging from the FAL-C model in which we have added a longitudinal magnetic field decreasing exponentially with height, from 200 G at the base of the photosphere to 40 G at the top of the chromosphere. The colored background in the same panels show the logarithm of the normalized contribution function for Stokes V, which gives an idea of the regions in the model atmosphere which contribute the most to the emergent circular polarization profile at each wavelength. The main contribution to the circular polarization of the spectral line at 259.608 nm comes from the photosphere, below the temperature minimum. The line at 262.147 nm forms at slightly larger heights, with significant contribution from the regions just above the temperature minimum. Finally, the contribution function of the resonance lines at 262.119 and 262.908 nm have their peak in the upper layers of the chromosphere, mainly around 1 Mm for the former, and even higher for the latter. The colored curves show the WFA fit to the theoretical circular polarization profiles. Because the contribution function of the 259.608 and 262.148 nm lines is more or less concentrated and coherent in sign at every wavelength, it is possible to find a good fit to the whole spectral range. The profiles are fitted with a magnetic field of 178 and 150 G, respectively. In the model atmosphere, these fields are found at heights ~ 0.2 and ~ 0.4 Mm, which correspond to approximately the middle of the region in the model with significant contribution function values (see colored background in the corresponding panels). For the resonant lines at 262.119 and 262.908 nm, the contribution function is significantly more extended and it changes sign with height at some wavelengths. For this reason, it is not possible to find a unique satisfactory fit to the whole spectral range (different regions of the profile are being affected by different magnetic fields, because they do not form in the same atmospheric region). We can fit the central part of the profiles with a magnetic field of 93 and 68 G for the two lines, respectively. These magnetic fields are found in the model atmosphere at heights ~ 1 and ~ 1.4 Mm, respectively, which also correspond to approximately those heights showing the largest value in the contribution function at the fitted wavelengths (see colored background in the corresponding panels). The WFA thus seem suitable for the quick inference of the longitudinal magnetic field at different layers of the solar atmosphere by combining the diagnostic of multiple Fe II with different formation regions.

5. SUMMARY AND CONCLUSIONS

We have theoretically investigated the formation of the intensity and polarization of the Fe II spectral lines in the relatively unexplored 250 - 278 nm window of the near-UV solar spectrum. We identified those lines for which we predict significant linear or circular polarization signals and investigated their magnetic sensitivity, as well as their suitability to infer the magnetic field in the solar atmosphere.

By means of NLTE RT calculations in a semi-empirical model of the solar atmosphere, we have obtained the Stokes profiles of the emergent spectral line radiation. To this end, we built a model atom with all possible transitions of interest in the above mentioned spectral region. Due to the lack of solar observations in this region of the solar spectrum, we use the observed intensity flux of α Cen A (a solar-like star) in order to adjust one of the most important and approximated parameters in our atomic model, namely the rate of inelastic collisions with electrons. We find that by reducing all these rates by a factor ten we obtain a theoretical flux very similar to the α Cen A observation at the core of the Fe II resonant lines. It is important to emphasize that this region of the spectrum is severely affected by the so-called UV blanketing, which we cannot accurately include in our modeling, and that is evident when comparing the

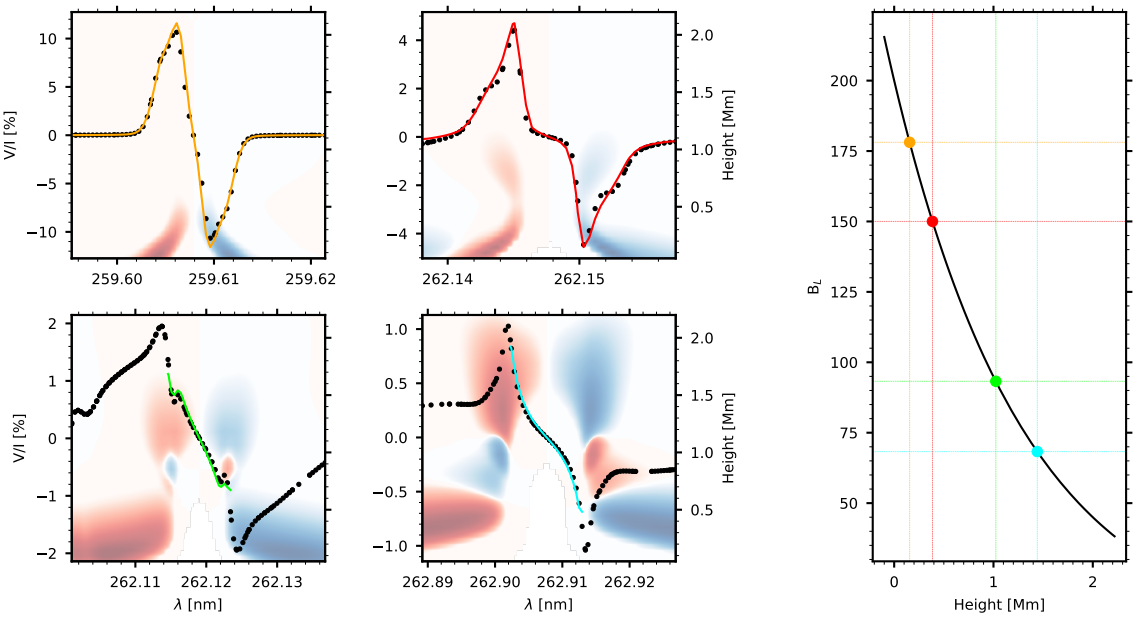

Figure 8. Emergent fractional circular polarization V/I (first and second columns) for the four selected lines (see Tab. 2) for a LOS at $\mu = 1$, calculated in the FAL-C model with a vertical magnetic field with an exponential stratification (see rightmost panel). The colored background shows the logarithm of the normalized contribution function for V/I (with the red and blue colors indicating positive and negative contributions, respectively). The colored curves in the first and second columns show the fit with the WFA. The colored circles in the right panel show the B_L value from the fit of the circular polarization profile for the curve of the same color, plotted at its intersection with the B_L stratification of the model. The colored lines in the right panel help to quickly identify the magnetic field and height values for each marker.

continuum level between the theoretical and observed flux profiles. While the impact of the UV blanketing, a priori, limits the diagnostic capabilities of the weaker lines and the wings of the strongest lines, the metallicity of α Cen A is considerably larger than that of the Sun. Therefore the impact of UV blanketing is expected to be less significant in the solar spectrum than in α Cen A. Future solar observations in this spectral window will make possible to study in detail how the UV blanketing affects the conclusions of this work and to further validate and improve the atomic data for the modeling of the Fe II spectral lines.

Most of the stronger (in intensity) Fe II lines do not show remarkable linear polarization signals for a close to the limb LOS ($\mu = 0.1$). Nevertheless, there are numerous lines with predicted signals with amplitudes larger than 0.2 %, and therefore we expect that they can be observed with spectropolarimetric instrumentation similar to that of CLASP2. We show the region of formation, critical Hanle field, and information about blends for all these lines. Most of them form around the middle chromosphere, with some forming in the upper chromosphere. We study in detail the magnetic sensitivity of the linear polarization of five of these lines, showing that those forming in the middle (upper) chromosphere are typically sensitive to magnetic fields with strength up to ~ 50 G (~ 20 G). These lines thus encode information about the expected weak magnetic fields in the chromosphere of the quiet Sun.

We find that, for a magnetic field strength of 50 G, more than a hundred Fe II transitions are predicted to show circular polarization signals above 0.5% strong enough to be able of use the WFA to reliably infer the longitudinal component of the magnetic field. We show the region of formation, effective Landé factor, and information about blends for all these lines. Most of them form in the upper photosphere and lower chromosphere, with some of them forming in the upper chromosphere. We estimate the order of magnitude of the magnetic field for which the WFA may not hold. We find that, for the lines forming in the photosphere, these values are mostly between 200 and 400 G, while in the middle and upper chromosphere the typical values are between 700 and 900 G. By applying the WFA to the theoretical circular polarization profiles of four lines with different heights of formation we are able to recover the magnetic field values of the imposed exponential stratification. When checking the height in the atmospheric model at which the inferred magnetic field is located, we can see that they coincide with the information provided by the circular polarization contribution function regarding the region of formation of each of the selected spectral lines.

The narrower 279.2 - 280.7 nm spectral window of the CLASP2 suborbital space experiment includes several spectral lines of already demonstrated utility for diagnosing the magnetic field across the whole solar chromosphere, namely the Mg II h and k lines and the resonance lines of Mn I. In addition, as we shall show in a forthcoming publication, it includes several other weaker spectral lines with measurable circular polarization signals in active region plages, such as two hitherto unexplored Fe II lines. The circular polarization of these Fe II lines provides information about the magnetic field which is complementary to the Mg II and Mn I lines in terms of the region of the atmosphere that they sample. All these near-UV lines of the CLASP2 spectral region are very suitable to map the magnetic field from the lower to the upper chromosphere. Nevertheless, the results of the present investigation on the magnetic sensitivity of the Fe II lines in the 250 - 278 nm spectral region, especially the prediction that they should show measurable circular polarization signals and sample different layers of the solar chromosphere when suitably combined, lead us to conclude that including these lines would further help determine the magnetic field throughout the whole solar chromosphere.

ACKNOWLEDGMENTS

We acknowledge the funding received from the European Research Council (ERC) under the European Union's Horizon 2020 research and innovation programme (ERC Advanced Grant agreement No 742265).

REFERENCES

Afonso Delgado, D., del Pino Alemán, T., & Trujillo Bueno, J. 2023, ApJ, 942, 60, doi: 10.3847/1538-4357/aca669

Allen, C. W. 1963, Astrophysical quantities (London: Univ. of London, Athlone Press)

Alsina Ballester, E., Belluzzi, L., & Trujillo Bueno, J. 2016, ApJL, 831, L15, doi: 10.3847/2041-8205/831/2/L15

Ayres, T. R. 2010, ApJS, 187, 149, doi: 10.1088/0067-0049/187/1/149

—. 2013, Astronomische Nachrichten, 334, 105, doi: 10.1002/asna.201211747

Belluzzi, L., & Trujillo Bueno, J. 2012, Astrophysical Journal Letters, 750, doi: 10.1088/2041-8205/750/1/L11

Belluzzi, L., Trujillo Bueno, J., & Štěpán, J. 2012, ApJL, 755, L2, doi: 10.1088/2041-8205/755/1/L2

Bely, O., & van Regemorter, H. 1970, ARA&A, 8, 329, doi: 10.1146/annurev.aa.08.090170.001553

Casini, R., Manso Sainz, R., & del Pino Alemán, T. 2017, ApJ, 850, 162, doi: 10.3847/1538-4357/aa9654

Cram, L. E., Rutten, R. J., & Lites, B. W. 1980, ApJ, 241, 374, doi: 10.1086/158350

De Pontieu, B., Title, A., & Carlsson, M. 2014, Science, 346, 315, doi: 10.1126/science.346.6207.315

De Pontieu, B., Polito, V., Hansteen, V., et al. 2021, SoPh, 296, 84, doi: 10.1007/s11207-021-01826-0

del Pino Alemán, T., Casini, R., & Manso Sainz, R. 2016, The Astrophysical Journal, 830, L24, doi: 10.3847/2041-8205/830/2/l24

del Pino Alemán, T., Trujillo Bueno, J., Casini, R., & Manso Sainz, R. 2020, The Astrophysical Journal, 891, 91, doi: 10.3847/1538-4357/ab6bc9

Fontenla, J. M., Avrett, E. H., & Loeser, R. 1993, ApJ, 406, 319, doi: 10.1086/172443

Ishikawa, R., Trujillo Bueno, J., Del Pino Aleman, T., et al. 2021, Science Advances, 7, 1, doi: 10.1126/sciadv.abe8406

Judge, P., Rempel, M., Ezzeddine, R., et al. 2021, ApJ, 917, 27, doi: 10.3847/1538-4357/ac081f

Judge, P. G., & Jordan, C. 1991, ApJS, 77, 75, doi: 10.1086/191599

Judge, P. G., Jordan, C., & Feldman, U. 1992, ApJ, 384, 613, doi: 10.1086/170903

Kano, R., Trujillo Bueno, J., Winebarger, A., et al. 2017, ApJL, 839, L10, doi: 10.3847/2041-8213/aa697f

Kobayashi, K., Kano, R., Trujillo Bueno, J., et al. 2012, in Astronomical Society of the Pacific Conference Series, Vol. 456, Fifth Hinode Science Meeting, ed. L. Golub, I. De Moortel, & T. Shimizu, 233

Kramida, A. 2013, in APS Meeting Abstracts, Vol. 2013, APS Division of Atomic, Molecular and Optical Physics Meeting Abstracts, D1.135

Kurucz, R. L., & Bell, B. 1995, Atomic line list

Lamb, F. K., & Ter Haar, D. 1971, PhR, 2, 253, doi: 10.1016/0370-1573(71)90011-1

Landi Degl'Innocenti, E., & Landolfi, M. 2004, Polarization in Spectral Lines, Vol. 307 (Dordrecht: Springer), doi: 10.1007/978-1-4020-2415-3

Li, H., del Pino Alemán, T., Trujillo Bueno, J., et al. 2023, arXiv e-prints, arXiv:2301.12792, doi: 10.48550/arXiv.2301.12792

Mihalas, D. 1978, Stellar atmospheres (San Francisco, CA: WH Freeman)

Rachmeler, L. A., Bueno, J. T., McKenzie, D. E., et al. 2022, ApJ, 936, 67, doi: 10.3847/1538-4357/ac83b8

Shchukina, N., & Trujillo Bueno, J. 2001, ApJ, 550, 970, doi: 10.1086/319789

Song, D., Ishikawa, R., Kano, R., et al. 2022, SoPh, 297, 135, doi: 10.1007/s11207-022-02064-8

Torres, C. A. O., Quast, G. R., da Silva, L., et al. 2006, A&A, 460, 695, doi: 10.1051/0004-6361:20065602

Trujillo Bueno, J. 2001, in Astronomical Society of the Pacific Conference Series, Vol. 236, Advanced Solar Polarimetry – Theory, Observation, and Instrumentation, ed. M. Sigwarth, 161, doi: 10.48550/arXiv.astro-ph/0202328

Trujillo Bueno, J., & del Pino Alemán, T. 2022, ARA&A, 60, 415, doi: 10.1146/annurev-astro-041122-031043

Trujillo Bueno, J., Štěpán, J., & Belluzzi, L. 2012, ApJL, 746, L9, doi: 10.1088/2041-8205/746/1/L9

Trujillo Bueno, J., Štěpán, J., & Casini, R. 2011, ApJL, 738, L11, doi: 10.1088/2041-8205/738/1/L11

Trujillo Bueno, J., Štěpán, J., Belluzzi, L., et al. 2018, ApJL, 866, L15, doi: 10.3847/2041-8213/aae25a

van Regemorter, H. 1962, ApJ, 136, 906, doi: 10.1086/147445

Watanabe, T., & Steenbock, W. 1986, A&A, 165, 163

Woodgate, B. E., Kimble, R. A., Bowers, C. W., et al. 1998, PASP, 110, 1183, doi: 10.1086/316243